May 2020

In Vitro Characterization of Shape Memory Polymer Foam Hemostats

Nakira Hollinae Christmas
Syracuse University

Abstract

Shape memory polymer foam hemostats are a promising option for future hemorrhage control in battlefield wounds. To enable their use as hemostatic devices they must be optimized in terms of formulation and architecture and characterized in terms of safety and efficacy. As a device advances through the stages of development, pre-clinical testing is required in animals. In order to help mitigate the excess use of animals as well as decrease the costs of pre-clinical research, relevant in vitro models need to be created and used for device optimization. In the work conducted here, two in vitro models were created; a simplified gunshot wound model and a grade V liver injury model were constructed and used for the testing of a variety of shape memory polymer foam hemostat geometries. The primary outcomes included how foam geometry affected wall pressures and hemorrhaging of the simulated blood. This work assisted in narrowing down hemostat design options based on the inflicted wound. After testing, the 8 different foam hemostat geometries pros and cons were elucidated, which will help to minimize future animal testing.

In Vitro Characterization of Shape Memory Polymer Foam Hemostats

by

Nakira Christmas

B.S., Syracuse University, 2019

Thesis
Submitted in partial fulfillment of the requirements for the degree of
Master of Science in Bioengineering.

Syracuse University
May 2020

Acknowledgements

Great appreciation is extended to the Mary Beth Monroe Lab of Syracuse University. I would like to thank Dr. Monroe for introducing me to a different way of thinking, innovating, and working. I have learned a lot from you and the members in our lab. I will forever cherish this experience as well as translate all you have given to me in the future careers or endeavors, I choose to embark on. Your tenacity for making learning fun, understandable, and streamlined has helped motivate me in an industry that can often feel like you are alone.

I would like to thank all my lab members for your constant support and grace. A special thank you to my two mentors, Anand Vakil and Henry Beaman, as well as my former mentees David Fikhman and Shi (Kat) Dong. The teamwork and immediate lessons that I both taught and learned has been priceless. Thank you for letting me know everything would happen just as it was expecting to.

A thank you also is awarded to the members who have agreed to serve on my thesis committee. Thank you, Dr. Mary Beth Monroe, Dr. James Henderson, Dr. Pranav Soman, and Dr. Alison E Patteson, for being of service to us students and helping us continue in our journey of learning.

Last, but not least, thank you to my family, friends, LSAMP research program, advisors, and classmates for your unwavering support in my dreams and goals. I have made it to the place that I am today due to your drive to assist me with moving towards success. I find this moment very serendipitous; it is almost surreal that it is happening.

#MommyWeDidIt!

Table of Contents

1. Introduction

1.1 Clinical Need: Uncontrolled Hemorrhage

Each year soldiers enter the battlefield with hopes of returning home to their families. Unfortunately, approximately 20% of combat casualties are killed in action (KIA), better known as killed before reaching treatment [2]. Uncontrolled hemorrhage is the leading cause of preventable death on the battlefield with 50% of the 20% of KIA soldiers dying from hemorrhaging [2]. Hemorrhage is loss of blood from a damaged blood vessel [4]. It can lead to a fluctuation in vital signs and an altered mental status as it progresses [4]. If hemorrhaging is not stopped, a person can possibly bleed to death in approximately five minutes [3]. If a person were able to recognize bleeding and apply more rapid and effective hemorrhage controlling agent, up to 16% of deaths on the battlefield would have preventable [5] Overall, hemorrhage claims ~1.5 million deaths per year [5], 30-50% [6] of which occur outside of the hospital.

1.2 Current Hemostat Solutions: Benefits and Drawbacks

Current hemorrhage controlling agents, or hemostats, include gauze, gauze with the assistance of a tourniquet, and a newer option, XStat®. Gauze has been in use since the 1890s [9]. There are two main types of medical gauze: woven and non-woven, in which they can be both sterile and non-sterile [10]. Woven gauze uses a loose open wave which helps fluid pass through the gauze and be absorbed by a more absorbable dressings (i.e. gauze pad or sponges). Non-woven gauze is created from fibers that appear to be woven but instead it is just more condense helping this type of dressing absorb more fluid. Non-woven gauze is often created with variations of ratios of

polyester or rayon, [10] which makes it one of the more comfortable wound dressings. Gauze has the capability of forming to any area, making it very useful for any traumatic wound injury. The downfalls of gauze, used alone, is that it is not as effective as other methods. It causes re-bleeds after removal, often places high pressure on the surrounding wall tissue especially when inserted into the wound and can be disruptive to wound healing since it dries and eventually can cause tissue damage when it is removed [11]. Tourniquets were first introduced in the battlefield in 1674 [12]. A solider wrapped a tight band below or above the site of the wound with the hopes of reducing pain and minimizing hemorrhaging by reducing blood flow to the wound [12]. Tourniquets used in conjunction gauze helps maximize the efficiency of gauze. The less blood that is flowing, the more the gauze can serve as a hemorrhage controlling hemostat at a rate of up to 7% [13]. Although tourniquets help with pain and blood control, they are intended to stop blood flow completely [13]. The tightness of the tourniquet is dependent upon the size of the limb. The tightness, appropriate application, and tourniquet type used (strap vs. pneumatic) determine the amount of time the tourniquet can be used. In the result that any are inappropriately applied, tourniquet use has a time sensitivity that can result in nerve damage [13], or in extreme cases, limb amputation. X-Stat® is a battlefield [8] hemostatic device built for wounds in the groin or axilla and narrow entrance extremity wounds that are unable to have tourniquets applied [7]. It consists of 3 sterile syringe applicators filled with ~92 pieces of cellulose expandable sponges with an absorbent animal-derived coating [8]. One application of sponges can absorb approximately 300 ml of blood totaling a maximum intake of ~900 ml of blood. [8] X-Stat® is limited in that it is a temporary device that can

only be used for up to four hours until surgical care can be given. [7] Within the four hours, all cellulose expandable sponges must be removed from the patient. They have been developing sponges that are detectable via X-ray [8] to help assist surgeons in removal, but that can lead to an increase in removal time and cost. Current methods have benefits of forming to any area, helping to reduce blood flow to the wound, and easy application. Cons of the current methods include limited effectivity and time sensitivity. With these current downfalls, there is a clinical need for a hemostat that can be effectively applied/removed, is biocompatible, causes rapid blood clotting to stop bleeding, and does not have a time sensitive removal window.

1.3 Shape Memory Polymer Foams

Shape memory polymers (SMPs) are smart materials that can maintain any type of shape with the assistance of an external stimuli (i.e. temperature). They can "remember" a primary and secondary shape in which the key to their "memory" is shape recovery. See **Figure 1** for an example showing a cycle of heating, deforming/molding, cooling and unloading [14]. The initial cycle creates the secondary shape. In order to initiate shape recovery, the heating stimuli is applied, allowing the SMP to recover to its original shape.

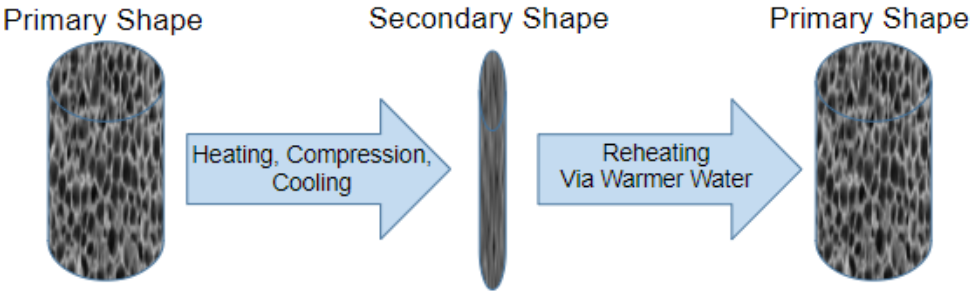

Figure 1. Primary and secondary SMP illustration.

SMP foams show great potential in hemostatic applications due to their high biocompatibility, high porosity, large surface area, and unique shape retention properties [15]. These foams have a highly porous shape that can compressed to a smaller volume in order to be inserted into any desired wound type. To fabricate SMP hemostats, foams are synthesized by mixing isocyanates and hydroxyls in traditional gas blowing processes. To prepare SMP foam hemostatic dressings, foams (1-2 liters) are cut into smaller sections, heated to their glass transition temperature, 45 to 70ºC in dry conditions [15], molded by compressing axially, and lastly cooled to lock in its secondary shape until it is ready to be applied to the bleeding wound. To tune the SMP glass transition temperature, the crosslink density of the network can be altered by varying ratios and end groups on isocyanate and hydroxyl monomers [15]. When the SMP is introduced to water, it causes plasticization, and the glass transition is reduced to below body temperature, based on network hydrophilicity and hydrogen bond disruption [16]. With the capability of tuning the glass transition temperature of a shape memory polymer foam hemostat, it permits the application of compressed foam(s) to deep and irregularly shaped wounds. Since wounds are at least the temperature for transition, the shape memory foam hemostats can expand back to their original shape forming to the shape of the wound, **see Figure 2.**

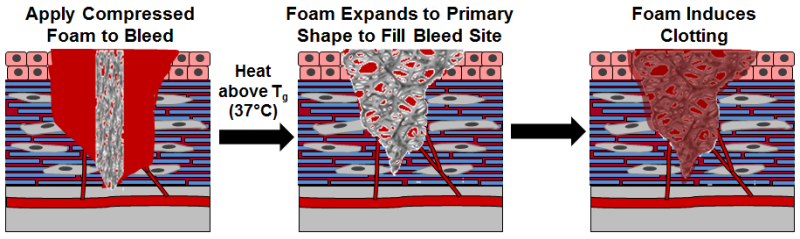

Figure 2. Shape memory polymer hemostat foam expansion in a bleed.

The characteristics of the foams that we are looking for is average pore size of ~1000 μm, a dry glass transition temperature > 50ºC, and a wet glass transition <37ºC.

SMP foams have been tested in in vivo aneurysms and peripheral vasculature that resulted in demonstrated biocompatibility [32] and rapid clotting [17] [18]. Porcine models were used to analyze the biocompatibility and thrombus formation characteristics of SMP foams over a 90-day period via histological evaluation [17] [32]. The polyurethane SMP foams demonstrated that they can apply minimal pressure to the walls of the wound, be highly biocompatible, and aid in the clotting in of blood. In the swine aneurysm model, biocompatibility was tested by analyzing the neointima formation across the aneurysm neck which isolated the aneurysm for the parent vessel without the compromise of the lumen. Biocompatibility was also shown by observing the inflammatory response in comparison to other suture materials (i.e. silk and polypropylene) [32]. The inflammatory response was minimal and that motivated the declaration of biocompatible polyurethane SMP foams. Thrombogenesis was evident through analyzing the endothelization and topography of the parent artery interface. As the days progressed from 0-90, the red blood cells followed the steps of thrombogenesis (blood cells forming along a parallel direction) and ultimately completely covered the aneurysms with endothelial cells [32]. In vivo polyurethane SMP foam studies produced data showing the combination of thrombogenic surface chemistry and high surface area-to-volume ratio results in rapid blood clotting within the foam [17] [18].

1.4 In Vitro Modeling

The SMP foam shows promise for addressing the current clinical needs but requires pre-clinical testing to demonstrate safety and efficacy. When creating a new medical device, it must go through pre-clinical testing processes set forth by the Food and Drug Administration (FDA) in order to be accepted into the market. In pre-clinical trials, in vivo studies are carried out on animals to predict how a device will perform in a human. It tests the safety and efficacy [24] of a device in order to declare that it is safe to use in humans. Approximately 26 million animals are used every year in the United States for scientific commercial testing [25]. Although animal testing can be very beneficial to the testing and regulation of a medical device, it has both benefits and limitations. Some benefits include real life characterization, testing is closer to the human body, demonstration of safety, a testing option when it is unethical to use human subjects, and animal life cycles are shorter enabling more rapid characterization of healing processes [25]. Some limitations include cost, loss of animal life, and differences between animals and humans [25] [26]. Thus, many devices and drugs that work in animals are not necessarily safe and effective in humans. In order to help mitigate the excess of animal testing, the creation and use of in vitro models is suggested [27].

1.4.1 Gun Shot Wound Model (Cylindrical Model)

A cylindrical in vitro model was created to simulate a gunshot wound based on the in vitro model experiment conducted by Kragh [33]. With the direction of literature, a mock circulatory system was set up around the 30 mm diameter x 70 mm length wound

cavity, molded in polydimethylsiloxane (PDMS), to measure the pressures on the bottom and side of the model. The fluid would come into the bottom of the model at a pressure of 100 mmHg based on the average blood pressure of humans. The liquid was gravity fed into the wound, and a 22% glycerol solution was used to simulate blood [19]. This model allowed for the packing of the hemostats as well as quantitative observations of fluid loss and pressures of the hemostats.

1.4.2 In Vitro Grade V Liver Wound Model

To provide more clinically relevant measurements, an in vitro grade V liver injury model was subsequently built and used for testing. A grade V liver injury model was selected since the liver is the most commonly injured abdominal organ that causes hemorrhagic death [28] [29]. The gunshot wound model was molded in PDMS, which has very different material properties than a liver. PDMS has an elastic modulus range of 0.57 MPa to 3.7 MPa [36] which is two orders of magnitude stiffer than human liver's elastic modulus range of 560 Pa to 720 Pa [37]. Using a new material with a modulus closer to the liver, ballistic gel was selected since it had an elastic modulus range of 121 kPa to 129 kPa [38]. The wound injury is characterized by the amount of lethal parenchymal damages along with major vascular lacerations. For an injury to be categorized as grade V, there must be at least two major blood vessels that have been cut, see **Figure 3** for reference [30] [31]. The fluid flow rate is used to simulate this study. In literature, a 35-45 kg pig has a liver size of ~1000g [34]. Since the constructed liver mold is smaller than that, using a 1:1 liver mass to fluid rate ratio [35], the flow rate could be calculated. In this in vitro model, we test the timing of application and removal, the effectiveness of clotting,

and the pressure on the wound walls after application of SMP foams in comparison with gauze and XStat® controls, similarly to in vivo testing in a gunshot wound model. The grade V liver injury model simulates porcine studies that are part of the pre-clinical trials for SMP foam hemostats.

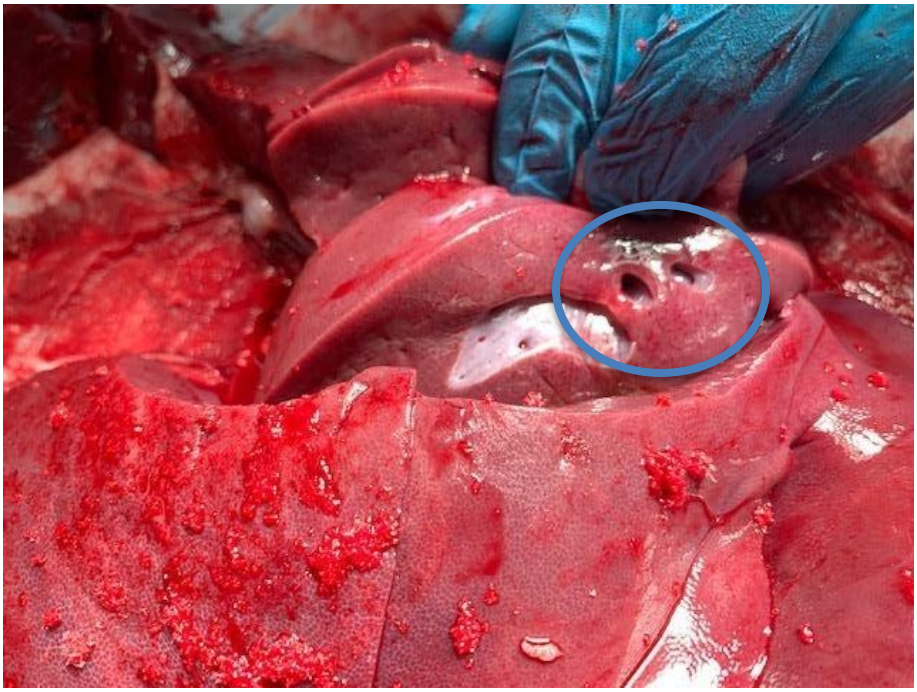

Figure 3. Liver showing the two lacerations of major blood vessels in order to classify a wound as grade V [photo by Henry Beaman, MBM LAB].

1.5 Research Overview

In this study, I looked at how SMP foam hemostats perform in different in vitro models that simulate real life battlefield wounds and animal models to maximize efficiency in pre-clinical trials. In the in vitro studies, I followed previous studies in the

literature that measure both side and bottom pressures, flow rate, fluid loss, and pressure on the walls.

1.5.1 Varying Foam Geometries

Shape memory polymers have the capability of being any shape or size. For wound packing hemostats, responders have the decision to use a standardized one size non-woven gauze roll or small pieces of cellulose X-stat® pieces. In a gauze vs X-Stat® study, the different geometries did not significantly alter bleeding rates and hemorrhaging, but the X-Stat® was favored for hemorrhage control [19]. By having different hemostatic geometries, it is expected that there will be changes in how packing will occur, the changes in wall pressure, and changes in how the hemorrhage is controlled. In order to increase hemorrhage control, wound packing should be maximized [20] [21] by standardizing application methods and reducing material rigidity while packing.

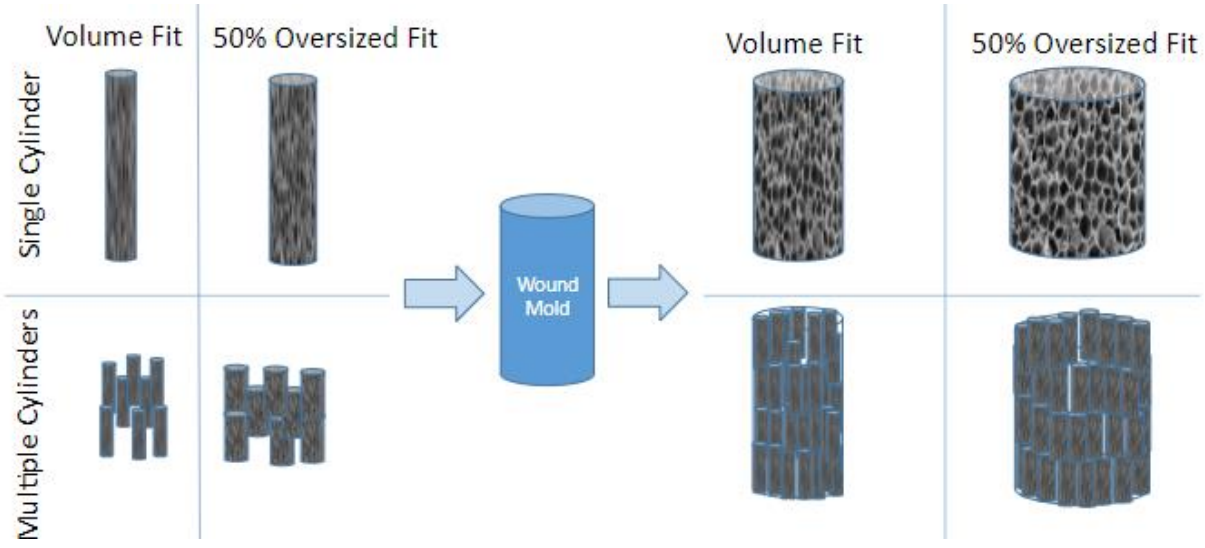

Figure 4. Different geometries and how they would fill the wound model.

The SMP foams in these studies were fabricated in analogous geometries to the gauze roll and X-Stat® (**Figure 4**). The single cylinders form a SMP hemostat in the size of a gauze roll while the multiple cylinders are like the smaller pieces of X-stat®. Using different geometries of one material helps improve understanding of wound packing and hemorrhage control in terms of wall pressures and fluid collection. An added foam geometry is shredded foam that serves as a SMP that can expand freely beyond the rigid primary forms of the single and multiple cylinders.

2. Methods

2.1 SMP Control Foam Synthesis

The control polyurethane foams were synthesized using the procedures described by Singhal et.al.[1] This process begins with an isocyanate (NCO) pre-polymer mix that contains hexamethylene diisocyanate (HDI) triethanolamine (TEA) and N,N,N',N'-tetrakis(2-hydroxypropyl) ethylenediamine (HPED). The NCO pre- polymer mix is prepared inside a glovebox and allowed to react for 48 hours at 50 ºC. After 48 hours, remove the (NCO) pre-polymer mixture and add surfactant. Allow the (NCO) pre-mix to cool while preparing the OH mixture/ The OH mixture is then prepared with (catalysts, TEA, HPED and deionized water (DI)). Once the OH mix is prepared and speed mixed using a high-speed mixer (FlackTek, Inc., Landrum, SC), The NCO and OH mixtures are combined and mixed using the high-speed mixture then it is poured into a 2 L beaker to allow for foaming. The foam is then placed to cured in a laboratory oven at 50 ºC for 5 to 10 minutes to ensure completion of the reaction then it is placed in the fume hood overnight.

2.2 Foam Characterization

2.2.1 Differential Scanning Calorimetry (DSC) Glass Transition Temperature

The glass transition temperature (T_g) was measured using a Q-200 DSC (TA Instruments, Inc., New Castle, DE). The foams T_g was observed under both wet and dry conditions. To measure dry T_g, foam samples were cut into pieces ranging from (3-5 mg). The data was collected by using the following process: 1.) Decreased

temperature to 0 °C at 10 °C min^{-1} and hold isothermal for 2 minutes, 2) Increased temperature to 80 °C at 10 °C min^{-1} and hold isothermal for 2 minutes, 3) Decreased temperature to 0 °C at 10 °C min^{-1} and hold isothermal for 2 minutes, and 4) Increased temperature to 80 °C at 10 °C min^{-1} and hold isothermal for 2 minutes. This created 4 cycles total, where dry T_g was then determined observing the second heating cycle.

Before conducting wet T_g measurement, foam samples (3-5 mg), were placed into a glass vial containing DI water. The vials were placed into the laboratory oven at 50 ºC for 15 minutes to fully plasticize. The samples were then removed from vials and patted dry using Kim wipes (Kimberly-Clark Worldwide, Inc.). The samples were placed into aluminum pans and covered with hermetic lids. The lids were then vented by inserting a small hole using a syringe needle. Using the Q-200 DSC, the same cycle program as dry T_g was utilized and the data was observed in the same heating cycle.

2.2.2 Scanning Electron Microscopy (SEM)

Foam pores were imaged using Joel NeoScope JCM-5000 Scanning Electron Microscope (SEM). Samples (1 cm^3) were cut and gold sputter coated for 45 seconds. Pore size was analyzed by a line drawn between the two farthest opposing pore walls using ImageJ.

2.2.3 Shape Memory Behavior: Volume Recovery Expansion Study

A water bath set to 37 ºC was prepared. Radially compressed foam miniature cylinders were prepared into compressed diameters which were measured via digital

calipers. Nickel titanium wire was threaded through the center of the sample and attached to the base plate of the water bath apparatus. The base plate was placed into the water bath and images were taken every 5 seconds for 5 minutes via go pro. The foam sample's diameter was re-measured after the 5-minute period using digital calipers. The images were analyzed using ImageJ where the foam diameter was measured for each individual image and scaled based on the initial and final measured diameters.

2.3 Foam Geometry Preparation

Foam samples were in the form of hot wire cut cylinders, hole punched cylinders and powder. The miniature cylinders (1.5 cm tall) were prepared using a wire cutter and a 1.5 cm diameter punch. The 100% cylinders (7 cm tall) were prepared using a wire cutter and a 3 cm diameter biscuit cutter punch. The 150% cylinders (7 cm tall) were prepared using a wire cutter and a 3.6 cm diameter biscuit cutter punch. Both 100% and 150% cylinders used the biscuit cutters as indentations to mark the diameter in which the wire cutter would cut along the vertical axis. For the powder, leftover punched 1.5cm cylindrical disks were used. The volume of one 1.5cm x 1.5cm punch was measured and the volume of the punched cylindrical disks was calculated finding the mass of the matching disk and calculating volume via the density formula (density=mass/volume). Cylinders and the cylindrical punched disks were cleaned using a 10X volume wash of 70% ethanol and 20X volume wash of deionized water. Each wash was done twice while on a shaker table for 5 minutes set at 100 rpm. Samples were then dried via vacuum oven at room temperature for 24 hours. Cylinders were heated to 70 ºC for 15

minutes and then placed into a radial crimper to prepare radially compressed samples. Foams remained in the crimper for 2 minutes at room temperature. Powders were made from cylindrical punched disks by blending in a standard kitchen ninja blender.

2.4 In Vitro Model Testing

2.4.1 22% Glycerol Formulation

22% glycerol mixture was created by measuring the volume of a glass container and calculating what 22% of the volume was for 99% pure glycerol addition. Once the glycerol was measured via a beaker and graduated cylinder and added to the container, then the remaining volume was filled using deionized water.

2.4.2 Gunshot (Cylindrical) Wound Model Fabrication and Data Collection

The cylindrical wound model starts with 3D printing a cylindrical wound shape with the dimensions of 3 cm diameter x 7 cm height (**Figures 5a, 5b, and 5c**).

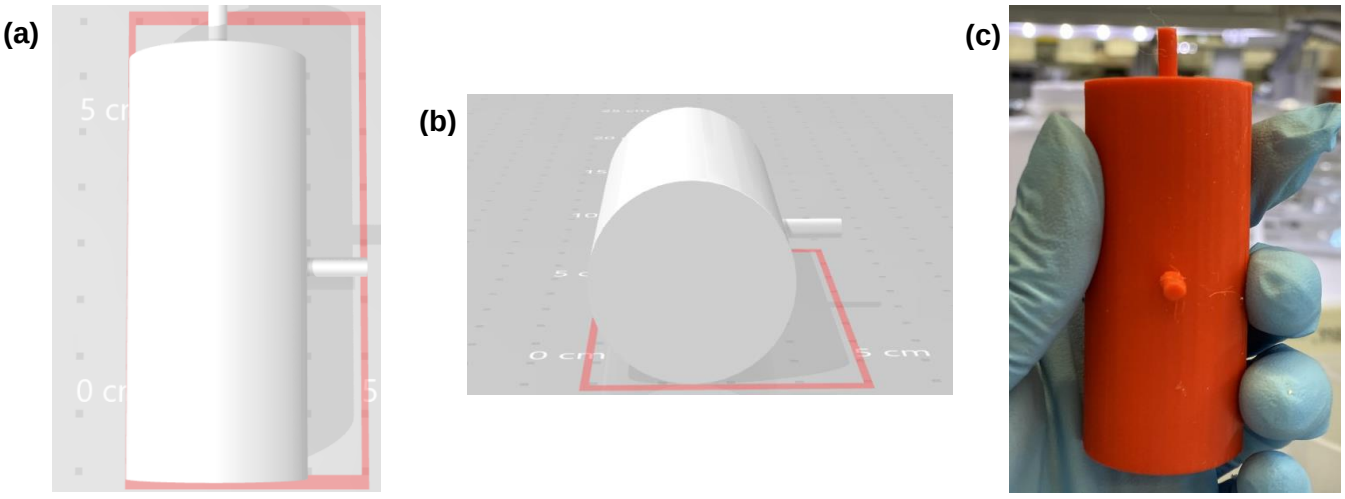

Figure 5. (a) And (b) IPT file of gunshot wound model and (c) Physical 3D print of gunshot wound model.

The model will also have small cylindrical inlets on the center of the side of the cylinder and the bottom with the dimensions of 0.3 cm diameter x 1 cm height once the model is 3D printed then the PDMS is created by mixing the elastomer and curing agent. Preheat a laboratory isothermal to approximately 100°C (~212°F). Once the PDMS mix is created, pour into a 250 mL beaker and add the 3D model in for setting. Cover the beaker with aluminum foil and allow it to set for 45 min to 1 hour. Remove the 3D model carefully and add silicon tubing to each inlet section. Attach one pressure gauge per inlet. The bottom inlet will have a T- connector in which one tube will be from the fluid reservoir and the other will go to the pressure gauge. Next place 7 ft. of tubing from the inlet to the T-connector, this is then connected to a stop cock. The stop cock is connected to another ft. of silicon tube which is then fed into a plastic 2 L square container in an insulating foam box. Data collection is the same for all foam geometries/hemostats. First heat 22% glycerol mix to ~37°C +/- 2°C. Add the fluids to the 2 L container in an insulated box and place on 2 L container on a 1.5 cm incline. Place the fluid reservoir and wound model at a height in which the silicon tubing is stretched its full length for the fluid to move via gravity. Set up a camera to record the run, also have a timer in the frame to help with data collection. Once the model is set up, measure the initial weight of the hemostat of choice. Next, observe the pressure via the pressure gauges prior to filling in fluids. Then, fill in the wound avoiding overflow and measure temperature then record. Turn on the camera and begin videotaping the trial. Add in the hemostat, begin timer, open stopcock and allow full fluid flow for 3 minutes. Once the 3 minutes ends, close the stop clock rapidly, and remove the hemostat. Measure the final weight of the hemostat, turn off camera, and measure the fluid in the

container (this is known as fluid loss). Repeat for all hemostats (i.e. gauze, X-stat®, different foam geometries). Data is then observed from the video by recording hemostat insertion and removal times, as well as side and bottom pressures of the wound every 15 seconds for the 3 minutes.

2.4.3 Grade V Liver In Vitro Model Fabrication and Data Collection

The ballistic gel grade V wound model starts with 3D printing a wound shape (see **Figures 6a and 6b**).

(a)

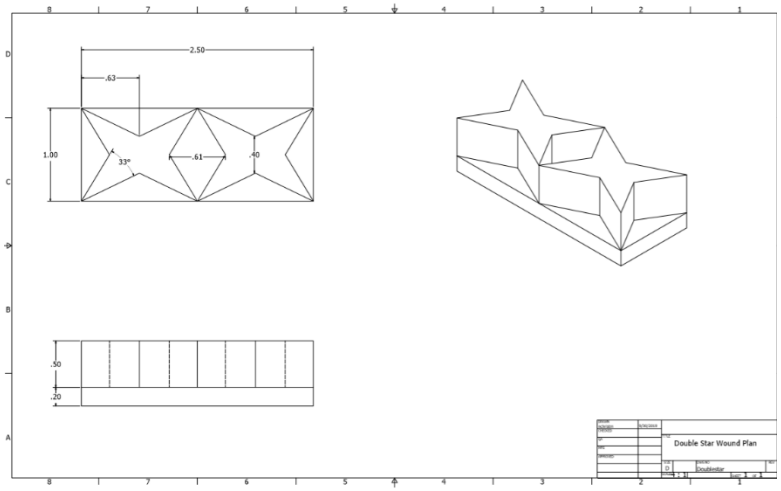

(b)

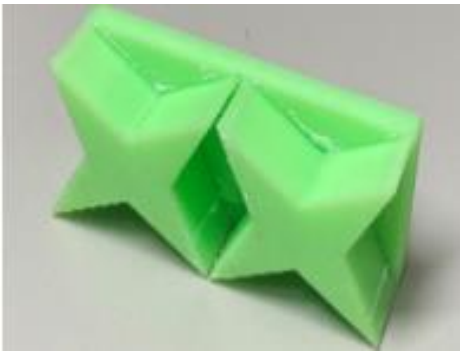

Figure 6. (a) Diagram of how the "Double Star" grade V model 3D model was made and (b) Physical Double Star 3D model.

Once the model is 3D printed then the ballistic gel is created by preheating a laboratory isothermal oven to approximately 120°C (~248°F) and placing gel into a 250 mL beaker. Cover the beaker with aluminum foil and allow it to melt for 3-4 hours. Once the gel is melted, pour the gel into a container sized (6.5 in length x 4 in width x 2 in depth) and place the 3D model completely into mold immediately. In order to push the model down further into gel and avoid rising, place 2 100g weights on both sides of the

model. Allow the model to set for 24 hours. Once the model is set, remove the model from the mold. Using wooden skewers, create holes at the marked location creating 4 holes for a grade V wound and measurement apparatuses (**Figure 7**).

Figure 7. The grade V model setup. X's mark where skewers were placed for fluid inlets/grade V cut (blue) and pressure outlets for measuring (orange).

Once the holes are created, fit silicon tubes safely through the holes so they are flush to the inside of the model. Attach one pressure gauge to the side tube where fluid is not entering, and one pressure gauge to tube flowing out of the bottom. Next, place 2 ft. of tubing into each of the remaining holes and attach the two free ends to a T-connector which is then connected to a peristaltic pump that is pumping the 22% glycerol fluid. In order to begin trials, heat 22% glycerol mix to ~31 +/- 2°C in a 2 L beaker. Place the fluid reservoir next to the peristaltic pump and insert the free end tubing that is fed through the pump into the glycerol. Set the peristaltic pump to 195 rpm

to simulate the flow rate of blood in a small porcine liver. Set up a camera to record the run, also have a timer in the frame to help with data collection. Once the model is set up, measure the initial weight of the hemostat of choice. Next, observe the pressure via the pressure gauges prior to filling in fluids. Then, fill in the wound avoiding overflow and measure temperature then record. Turn on the camera and begin videotaping the trial. Add in the hemostat, begin timer, start the peristaltic pump and allow full fluid flow for 3 minutes. Once the 3 minutes ends, stop the peristaltic pump, and remove the hemostat. Measure the final weight of the hemostat, turn off camera, and measure the fluid in the container (this is known as hemorrhage/fluid loss). Repeat for all hemostats (i.e. X-stat® and different foam geometries). Data is then observed from the video by recording hemostat insertion and removal times, as well as side and bottom pressures of the wound every 15 seconds for the 3 minutes.

3. Results and Discussion

3.1 Foam Characterization

3.1.1 Glass Transition Temperature

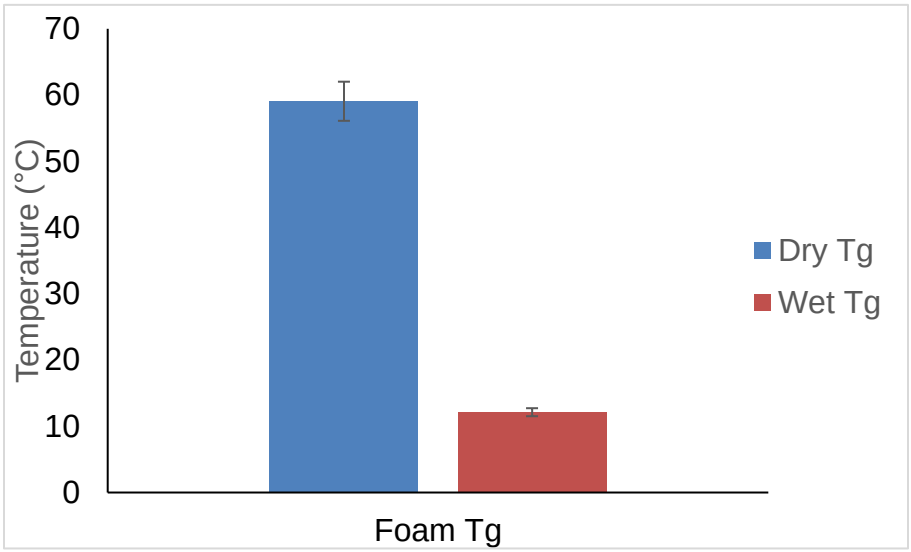

Figure 8. Average glass transition temperatures based on the state of the control foam

3.1.2 Pore size

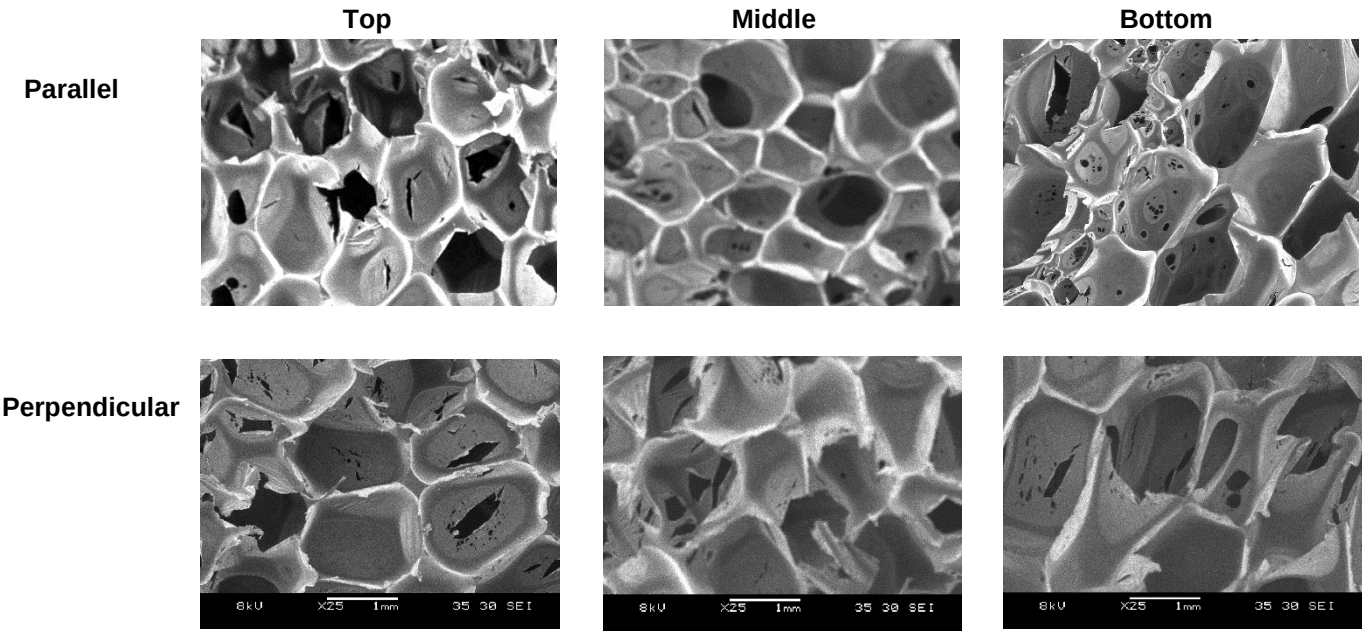

Figure 9. SEM images to show the pores of the formulated control foams.

3.1.3 Shape Memory Behavior: Volume Recovery Expansion

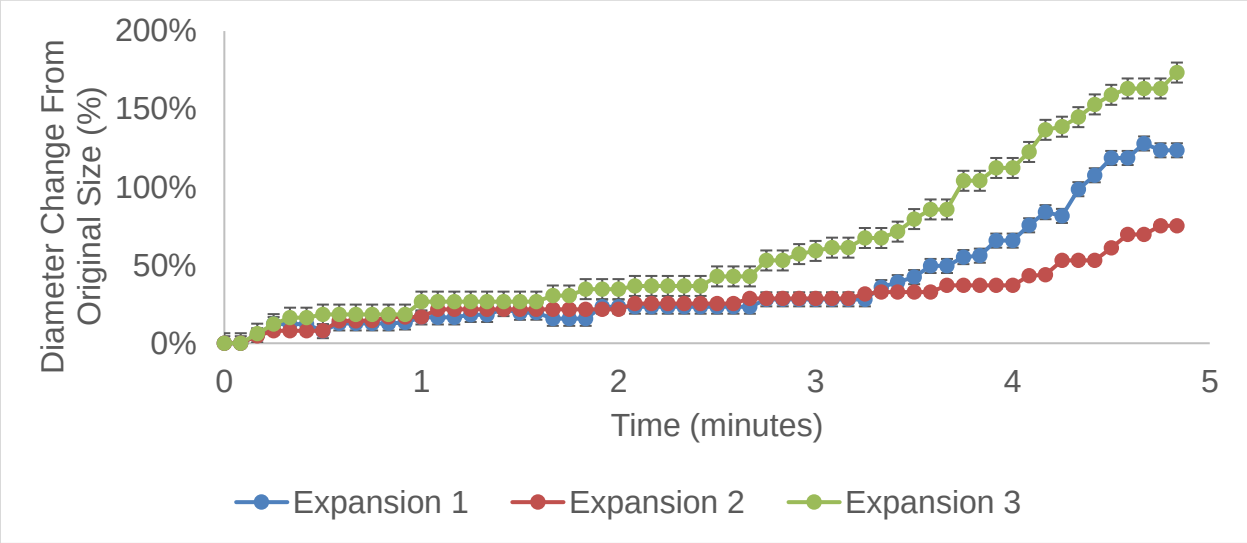

Figure 10. Volume recovery of a crimped SMP foam.

3.1.4 Final Geometries

(a)

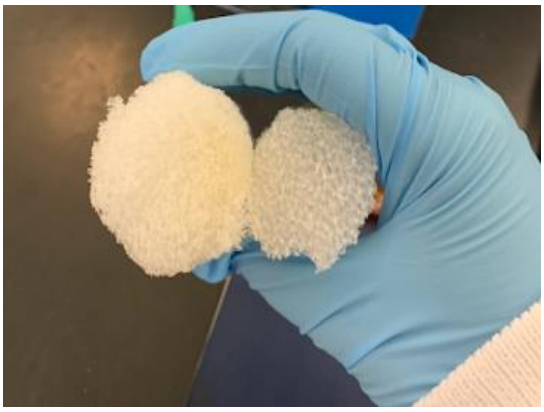

(b)

(c)

Figure 11. (a) 150% and 100% single cylinder foam, (b) Small Foams for 100% and 150% fill, and (c) Shredded foams loaded in syringes.

The control foams that were synthesized matched the hemostat design criteria. The average dry T_g was 59.06 ± 2.72 °C (**Figure 8**) and the average wet T_g was 12.12 ± 0.92 °C (**Figure 8**). A dry T_g of >50°C and wet T_g of <37°C was desired. The dry T_g criterion was important because it showed the control formulation would be able to be crimped and stably stored without premature actuation at extreme battlefield temperatures. The reduced wet T_g is required for actuation upon exposure to water in blood at body temperature upon implantation. The gunshot in vitro model trials were run at ~37°C and the grade V in vitro model trials were run at ~31°C. and it was desired that the foams actuate as soon as possible to help control hemorrhaging of the glycerol solution. The SEM images show an average pore size of 1177 ± 300 µm, which was within the criterion of pores of ~1000 µm (**Figure 9**) to enable foam crimping. In the volume recovery study (**Figure 10**), the average expansion percentage after 5 minutes in 37°C water was 124 ± 49 %. The rapid actuation enables filling of the wounds. After ensuring that foams met all design criterion, the different foam geometries were constructed in order to test the different forms of hemostats. **Figure 11** shows that the foams could be fabricated in different geometries and demonstrates the versatility of this material. The 150% cylinder diameters were ~4.5 cm and the 100% diameters were ~3.0 cm. For the small cylinder fill, a variety of small foams were made and separated out in order to conduct the trials. The 150% fill required 21 cylinders and the 100% fill required 14 cylinders. Lastly, syringes were filled with finely grated foams and had the density of ~0.83 g/mL. The control foams maintained their integrity during fabrication, testing, and cleaning. The same samples were using in multiple trials.

3.2 Gunshot Wound Model

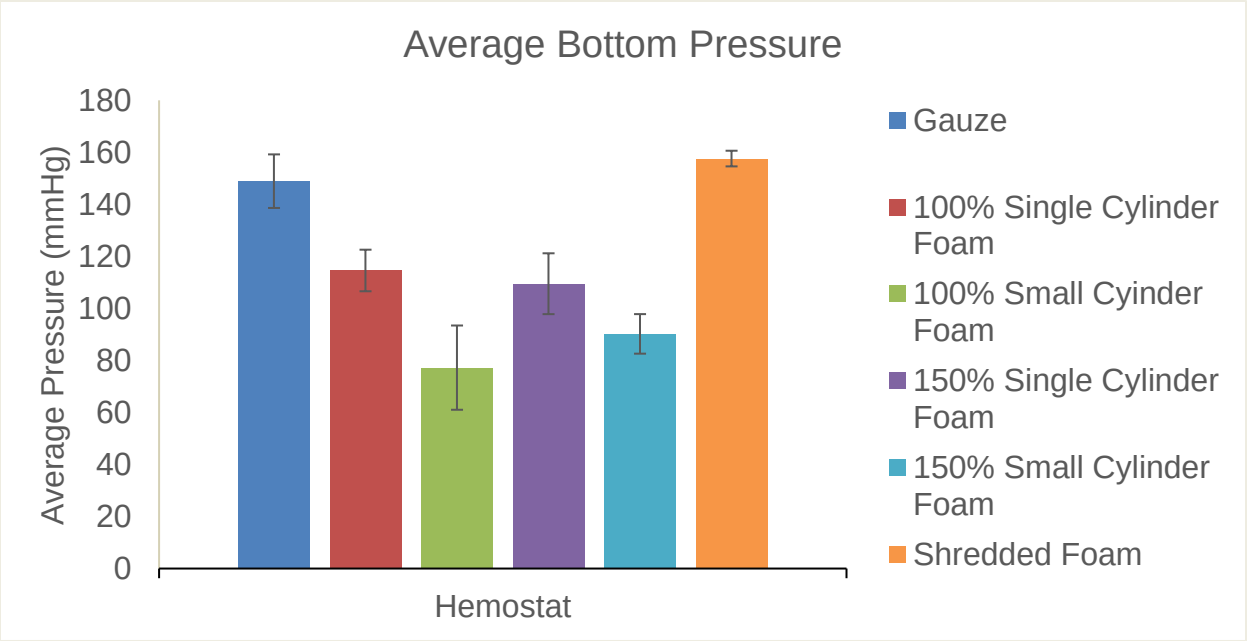

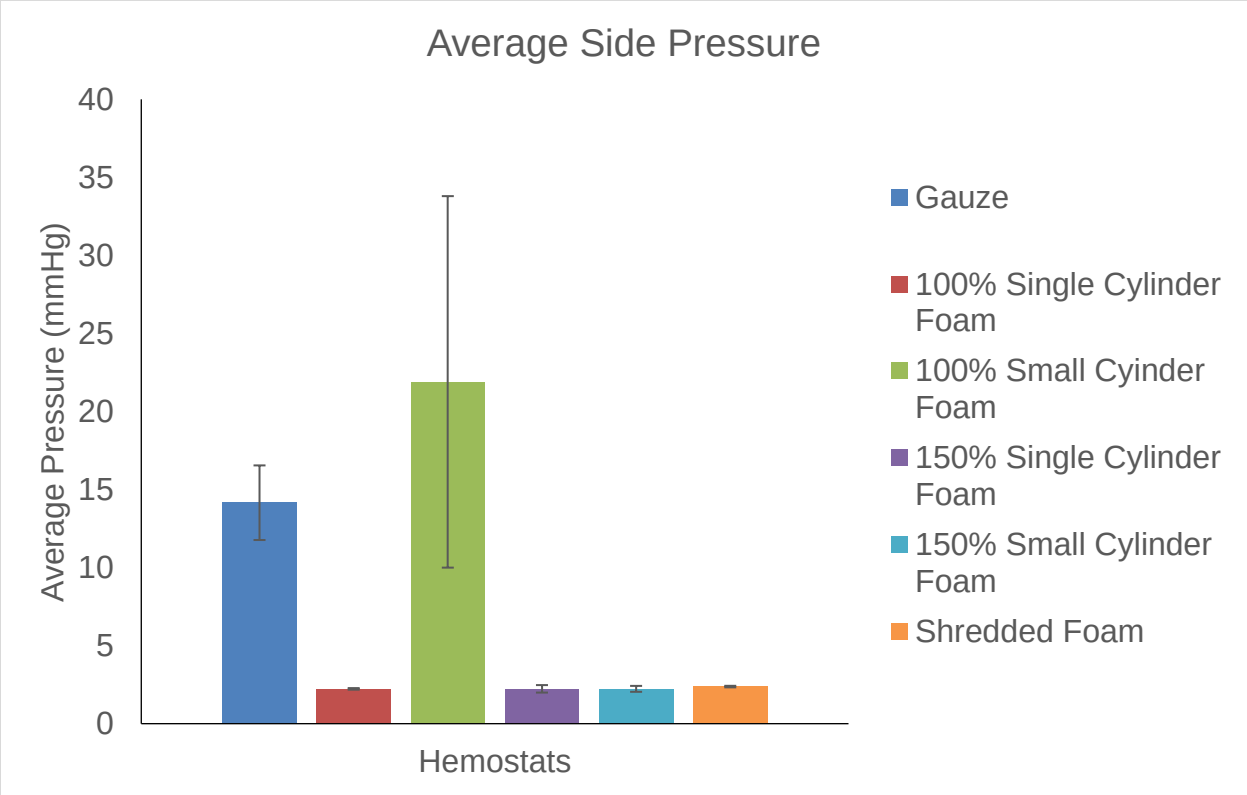

Figure 12. Average pressure of each hemostat in gunshot model

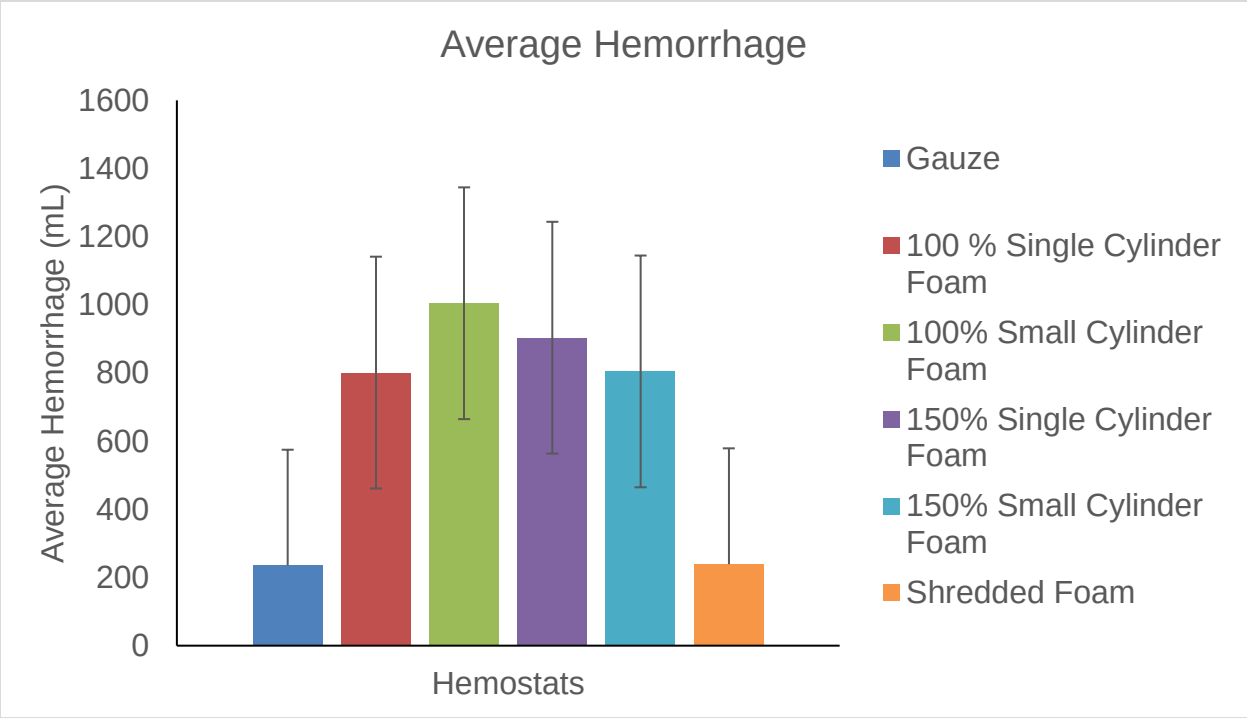

Figure 13. Average hemorrhage volume of each hemostat in gunshot model

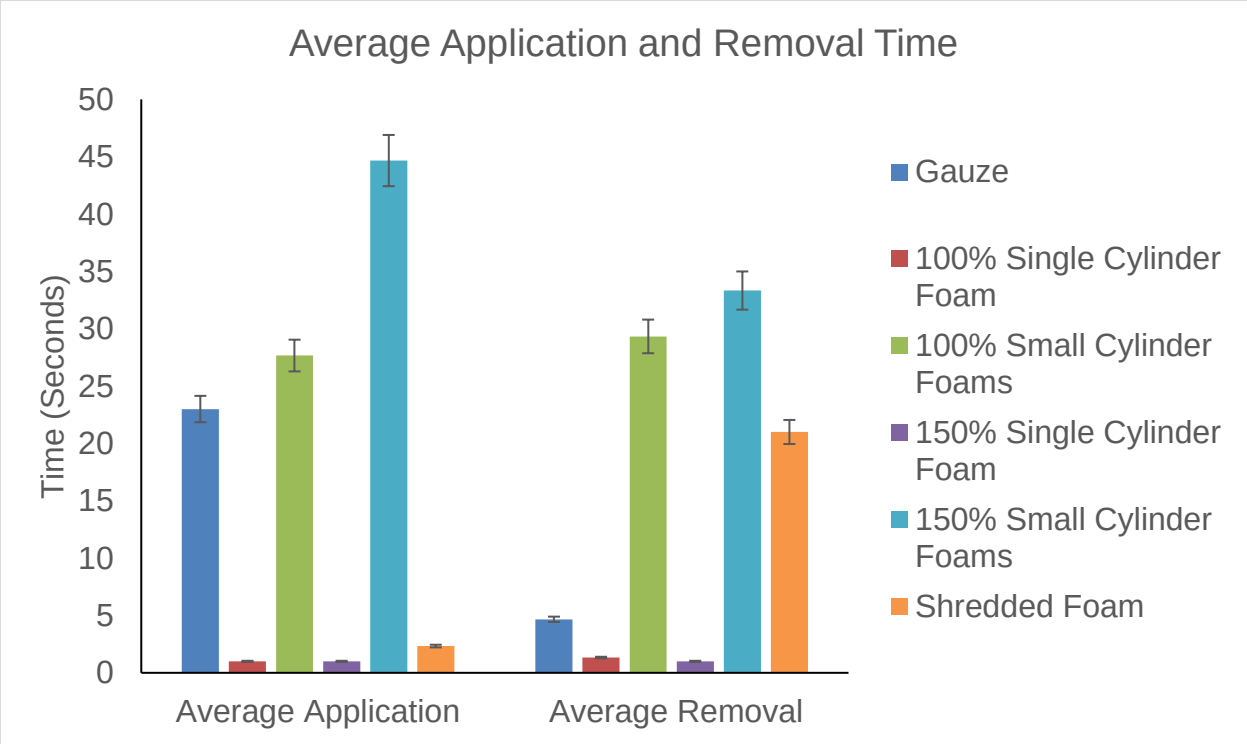

Figure 14. Average application/removal time per hemostat in gunshot model.

The gauze fill hemostat data in the cylindrical gunshot wound, **Figure 12**, showed that the average bottom pressure was much higher than the average side wall pressure. The average bottom pressure was 149 ± 10 mmHg and the side pressure were 14 ± 2 mmHg. This was to be expected due to the blood flow coming into the model from the bottom. The 22% glycerol and water mixture had to push through the bottom of the gauze in order to leave the wound. With the gauze being tightly packed into the model, it induced more pressure. The sides maintained lower pressure because no fluids were entering from that location, it was only the fluid buildup within the gauze that would affect that pressure as it was what was pushing against the walls. Gauze was exceptional for controlling the fluid loss as it had an average hemorrhage of 235 ± 49 mL (**Figure 13**).

The 100% and 150% SMP single cylinder fill followed the same trend in having higher bottom pressure in comparison to side pressure. The difference between the gauze and the SMP hemostat was that the foam hemostat needed time to expand and the pressures on both the bottom and the side were much lower. While the foam was expanding, it was putting little to no pressure on the side walls and it was allowing a lot more fluid to be lost because there was free space for the glycerol mixture to move. The average pressure for the bottom of the 100% single cylinder fill was 77 ± 16 mmHg and the average pressure for the side was 22 ± 12 mmHg (**Figure 12)**. The average pressure for the bottom of the 150% single cylinder fill was 109 ± 12 mmHg and the average side pressure was 2.1 ± 0.2 mmHg (**Figure 12**). The 100% and 150% single cylinders had a difference in hemorrhage volume. The averages were 801 ± 103 mL and 904 ± 69 mL, respectively (**Figure 13**). There is a large increase in pressure on the

bottom of the model between the two fills because the 150% fill has a larger circumference to actuate and combat the pressure of the glycerol mixture. The side pressures were very different because of how the water actuates with the hemostats. Since the 100% single cylinder is smaller and has less crimped material, it is easier for the water to enter and expand the foam faster. In comparison, it took a lot longer for the 150% single fill cylinder to fill reducing wall contact for a large amount of time in the trials. Since it took longer for the larger foam to actuate, it had an increased average fluid loss, indicating that the 100% fill hemostat may be preferred. In order to improve these trials, increasing the temperature to ~37 °C would help cause faster actuation of both and potentially give the 150% single cylinder the opportunity to expand more and perform more hemorrhage control.

The 100% small cylinder fill and 150% small cylinder fill followed the same bottom and side average pressure, but they had an even bigger gap with the amount of fluid loss. Using the smaller foams allowed for an opportunity to better pack the wound but it also took a lot more time in comparison to both the gauze and single cylinder fills. The average bottom pressure for the 100% small cylinder fill was 77 ± 16 mmHg, and the average side pressure was 22 ± 12 mmHg (**Figure 12**). The average bottom pressure for the 150% small cylinder fill was 90 ± 8 mmHg, and the average side pressure was 2.2 ± 0.2 mmHg (**Figure 12**), The pressures followed the same pattern of the single cylinder fill where the 150% size placed more pressure on the bottom, but not the side. The reasoning for that is similar; there is more packing, but it is harder for the water to reach all pieces of foam to enable actuation. Due to the 100% small cylinder fill having more spaces and not being as tightly packed as the 150% small cylinder fill, the

100% small cylinder fill lost a lot of fluid. The average fluid loss for the two geometries were 1005 ± 44 mL and 805 ± 108 mL, respectively (**Figure 13**). The 100% small cylinder fill lost the most fluid in comparison to all other hemostats tested, which is attributed to reduce wound packing.

The shredded foams were the most remarkable of all the hemostats. Their performance was what was expected of the other hemostats. The shredded foams placed a lot of pressure on the bottom of the wound, which is wanted to stop the bleeding, and very minimal pressure on the sides. The average bottom pressure for the shredded foams was 158 ± 3 mmHg and the average side pressure was 2 ± 1 mmHg (**Figure 12**). With the foam being free to move and very small, enabling almost immediate expansion, it reduced the fluid loss. The average fluid loss was 239 ± 53 mL (**Figure 13**), which was the smallest amount loss throughout the entire gunshot wound study.

Using the smaller foams allowed for an opportunity to better pack the wound but it also took a lot more time in comparison to both the gauze, single cylinder fills and shredded foam. It took approximately 25 seconds to insert the gauze, about 1 second to put in the both diameters of compressed single cylinders, about 3 seconds to push in shredded foam, and about 30-45 seconds to properly pack the number of cylinders required for the trial (**Figure 14**). For removal time, it took approximately 5 seconds for gauze, 2 seconds for the compressed cylinders, 30-35 seconds for small cylinders and 20 seconds for the shredded foam (**Figure 14**). This study indicates that it would be better to use the shredded foam when testing in gunshot wound related animal studies.

3.3 Grade V Liver Injury Model

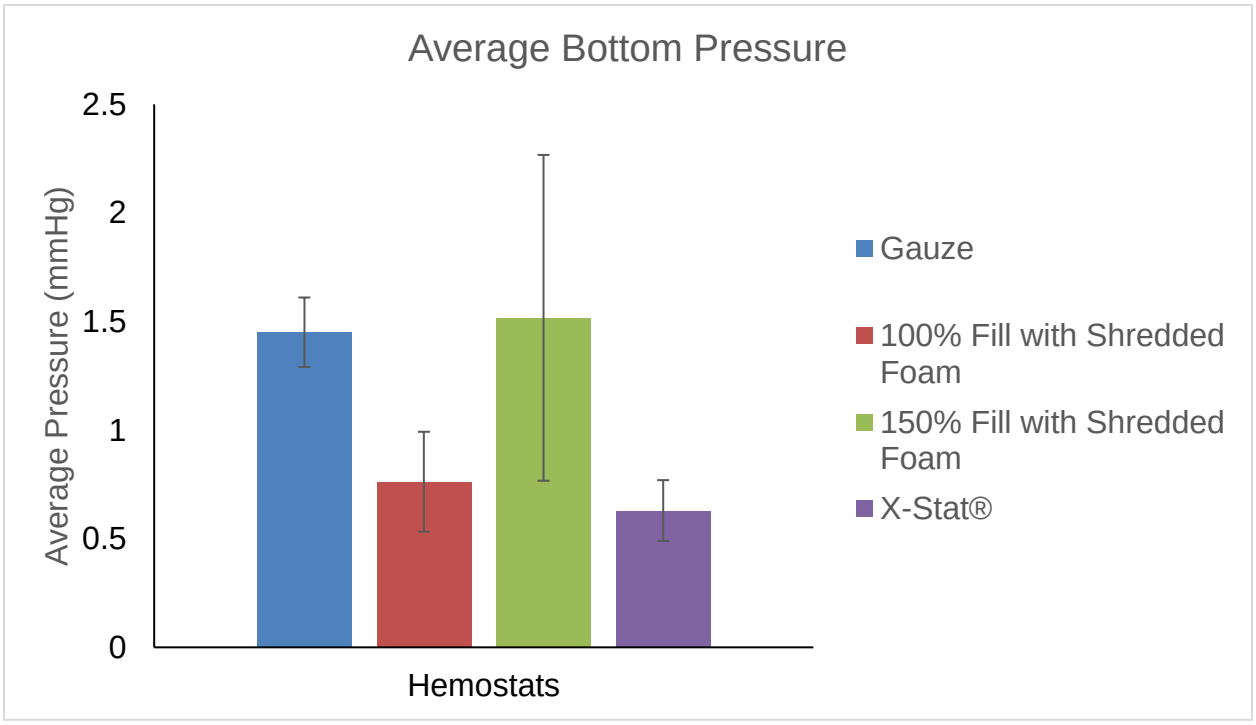

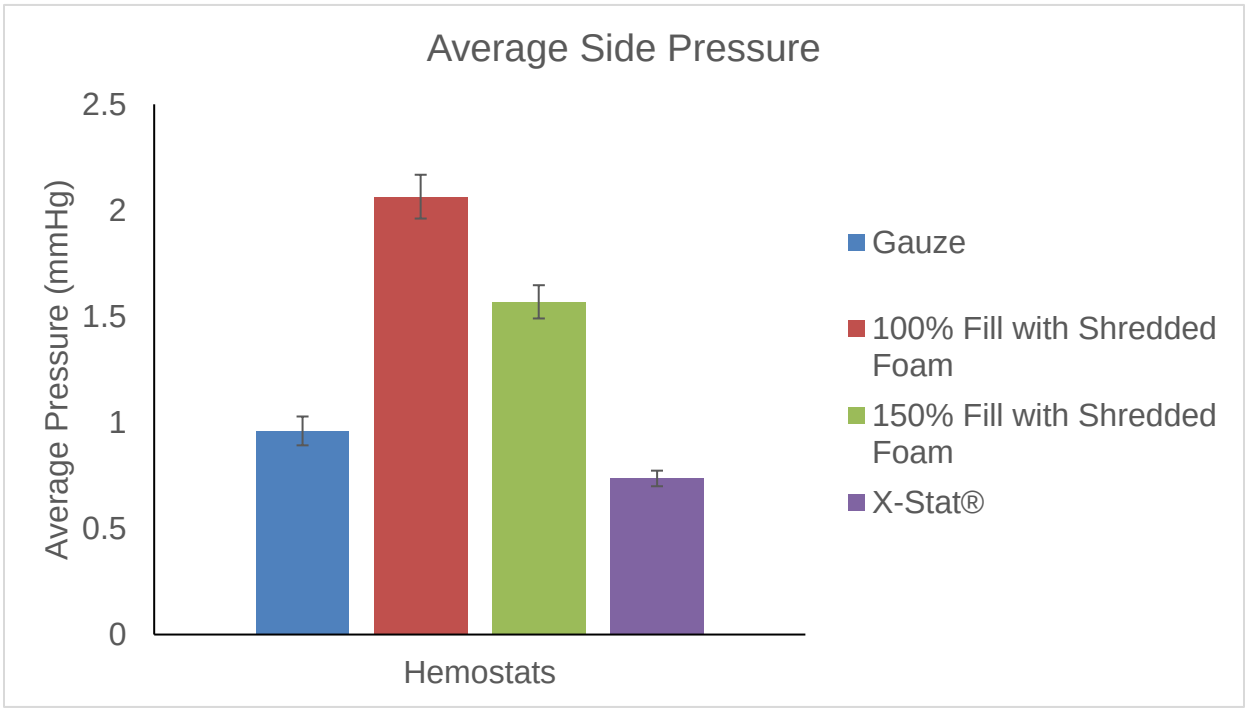

Figure 15. Average pressure of each hemostat in grade V model

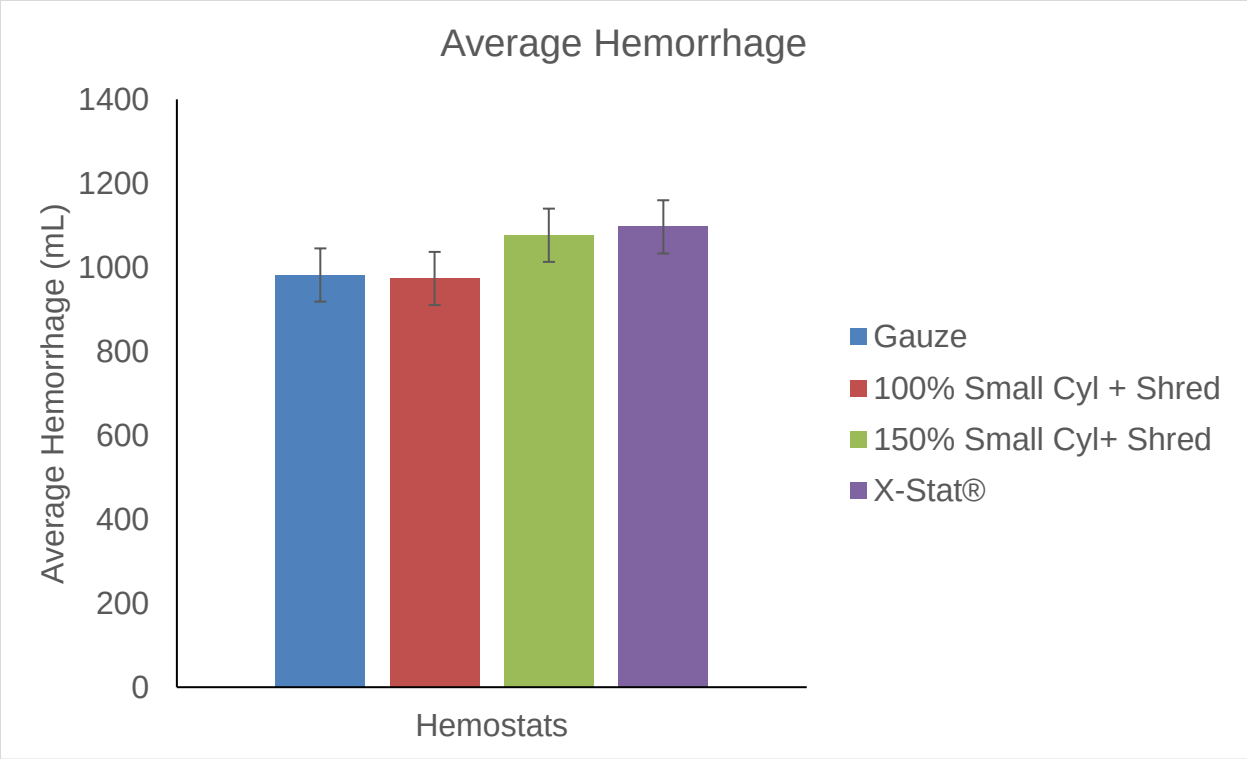

Figure 16. Average hemorrhage per hemostat in grade V in vitro model.

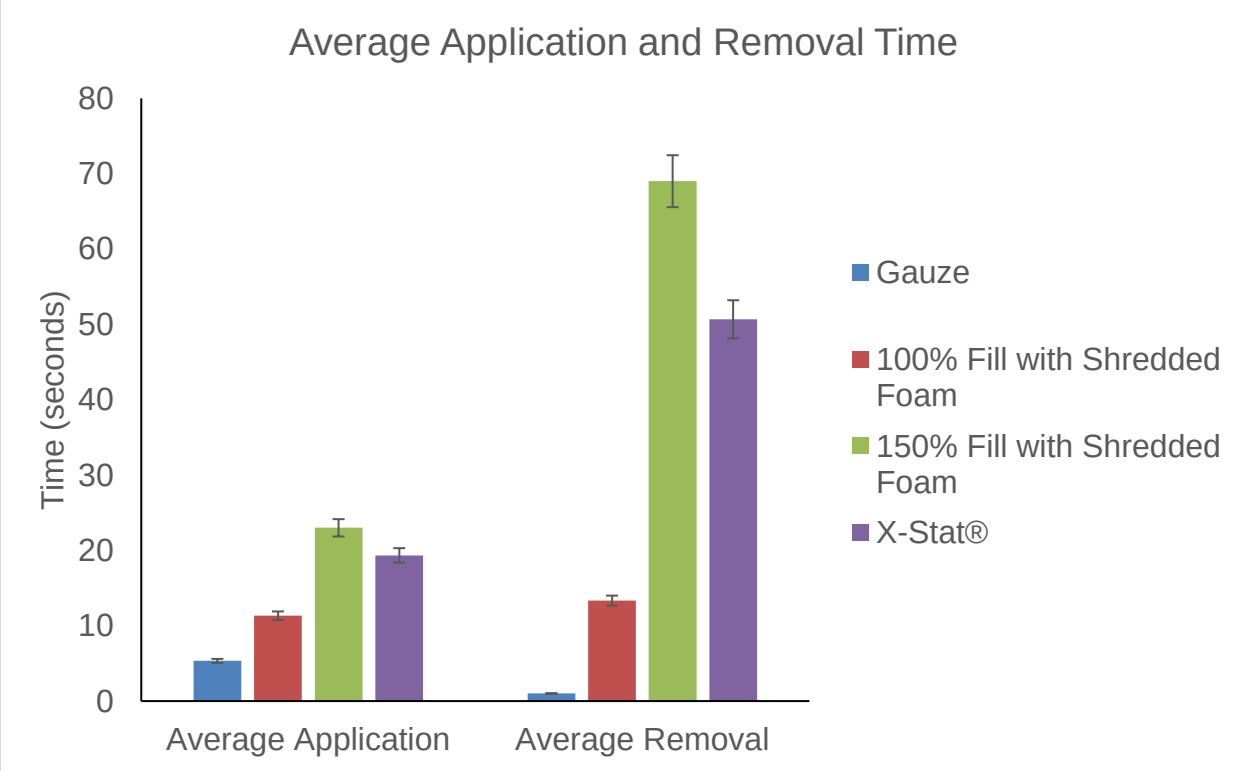

Figure 17. Average application/removal time per hemostat in grade V in vitro model.

The grade V liver injury in vitro model was designed to be more relevant for the intended animal model in pigs. The ballistic gel material is more flexible in comparison to the rigid PDMS gunshot wound model, which played a role in the massive decrease in the average pressures overall. Based on the gunshot wound model data, the smaller cylinders were combined with shredded foam to enable efficient packing of the larger wound volume. The grade V model required more intricate packing in respect to the gunshot wound model. Thus, the small cylinders were used to fill the bulk of the volume, and the shredded foam was used to assist with the reduction of hemorrhage. Before beginning the hemostat trials, a series of gauze trials were conducted, and the average bottom pressure was 1.5 ± 0.2 mmHg. The side pressure, as expected, was lower and it was 1.0 ± 0.1 mmHg (**Figure 15**). Gauze did an exceptional job of filling the wound and preventing massive fluid loss. The average fluid loss for the gauze trials was 982 ± 52 mL (**Figure 16)**. From the gauze trials, it was hypothesized that the grade V liver injury model would follow the same pattern of always having a higher bottom pressure, but that was not the case.

The hybrid of 100% small cylinder fill and a tube of shredded foams showed the opposite trend; the average bottom pressure was 0.8 ± 0.2 mmHg, and the average side pressure was 2.1 ± 0.8 mmHg (**Figure 15**). The model was ideally packed, and the hemorrhage loss was around the same as the gauze. It was expected that it would be the same because they packed the wound approximately the same way. The average fluid loss for the 100% small cylinder and shredded foam trials was 973 ± 16 mL (**Figure 16**).

The 150% small cylinder fill and a tube of shredded foams had comparable pressures to the 100% hybrid. The average bottom pressure was 1.5 ± 0.8 mmHg and the average side pressure was 1.6 ± 0.3 mmHg (**Figure 15**). For the same pressures approximately being applied, the 150% hybrid lost approximately 100 more mL of the glycerol mix in comparison to both the gauze and the 100% hybrid. The average hemorrhage for these trials was 1076 ± 81 mL (**Figure 16**).

X-Stat® in comparison to all hemostats, performed opposite of expected. The bottom and side pressures were not extremely different although they were lower, but the hemorrhage loss as well as the actual performance of X-Stat® explains why it produced the results that it did. X-Stat® produced an average bottom pressure of 0.6 ± 0.1 mmHg and an average side pressure of 0.7 ± 0.4 mmHg (**Figure 15**). The plausible reason that the pressures were as low is due to the way that X-Stat® packed the wound. The small pieces would go into the wound and expand greatly in comparison to their original length in order to soak in the fluid. As the pieces rapidly expanded, they pushed other pieces out of the wound and left a lot of gaps which allowed massive fluid loss. This hemostat had the greatest average fluid loss of all trials, 1096 ± 224 mL (**Figure 16)**. This data indicates that X-Stat® is better for wounds that are deeper. In the grade V liver injury in vitro model, horizontal packing was more important than the vertical packing required in the gunshot wound model.

Like the gunshot wound model, using the smaller foams allowed for an opportunity to better pack the wound with the assistance of the shredded foam. It took approximately 5 seconds to insert the gauze, about 1 second to put in the both diameters of compressed single cylinders, about 3 seconds to push in shredded foam,

and about 30-45 seconds to properly pack the number of cylinders required for the trial (**Figure 17**). For removal time, it took approximately 1 seconds for gauze, 2 seconds for the compressed cylinders, 30-35 seconds for small cylinders and 20 seconds for the shredded foam (**Figure 17**). This study indicates that it would be better to use the 100% small foam fill and shredded foam when testing in this sized wound.

4. Conclusions

The series of tests conducted here with a gunshot wound model and a grade V liver injury model can enable reduction in future animal studies. In vitro models can be tuned to different wound types, and desired measurements can be designed into the model. In our case, we were heavily focused on the pressure that the hemostats place on the walls and the fluid that is lost after hemostat application. Understanding pressure helps us gauge if there would be any damage to the surrounding tissues after application. Understanding fluid loss helps us tune the hemostats to better control hemorrhaging before wasting the life of an animal.

Full size single cylinders shall not be removed from the study when gunshot wounds are tested because they are easier to use for both application and removal. The cylinders showed that they can mold to the shape of the wound while also covering a lot of surface area. From the data obtained here, it is evident that over packing a wound does not promise an improvement in hemorrhage control. For future clinical trials, it would be advised to use the hybrid hemostats of small cylinders and shredded foam that fit the wound more efficiently to avoid hemostat migration. Another observation of wound packing is to ensure that the highest pressure of the hemostat is applied to the wall where the fluid is coming into. With that control, fluid will hypothetically have a greater challenge of escaping the wound and causing massive hemorrhaging.

Overall, the construction of in vitro models is very important to the effective advancement of medical devices. Each hemostat formulation provided new information that will be able to be used to optimize future in vivo pre-clinical trials. The established models can be used in future studies to assess alternate geometries and foam formulations based on the shape of the wound created.

References

[1] Allison, H. A. (2019). Hemorrhage Control: Lessons Learned from the Battlefield Use of Hemostatic Agents That Can Be Applied in a Hospital Setting. *Critical Care Nursing Quarterly*, *42*(2), 165–172. https://doi.org/10.1097/CNQ.0000000000000249

[2] Cannon, J. W. (2018). Hemorrhagic Shock. *New England Journal of Medicine*, *378*(4), 370–379. https://doi.org/10.1056/NEJMra1705649

[3] Alam, H. B., Col, † ;, Burris, D., Usa, M. C., Lcdr, ;, & Dacorta, J. A. (2005). Hemorrhage Control in the Battlefield: Role of New Hemostatic Agents. In *MILITARY MEDICINE* (Vol. 170). Retrieved from www.hemcon.com

[4] Ladlow, J. (2017). Hemorrhage. In *Complications in Small Animal Surgery* (pp. 72–78). https://doi.org/10.1002/9781119421344.ch12

[5] Kauvar, et al. J. Traum. Acute Care Surg. (2006); Markenson et al. Circulation. (2010); Petersen et al. Expert Rev Anti Infect Ther. 2011

[6] Tien HC, Spencer F, Tremblay LN, et al. J Trauma. 2007;62(1):142–146.

[7] Company, X.-S. (n.d.). XStat – RevMedx. Retrieved April 8, 2020, from https://www.revmedx.com/xstat/

[8] Administration, F. and D. (n.d.). *DE NOVO CLASSIFICATION REQUEST FOR XSTAT*.

[9] Dhivya, S., Vijaya Padma, V., & Santhini, E. (2015). *Wound dressings-a review*. *5*(4), 24–28. https://doi.org/10.7603/s40681-015-0022-9

[10] Medicine, E. (2018). Express Medical Supply Blog | Medical Gauze Guide. Retrieved April 8, 2020, from https://www.exmed.net/blog/expressmedicalsupply/post/2018/10/25/medical-gauze-guide.aspx

[11] Jones, V., Grey, J. E., & Harding, K. G. (n.d.). *ABC of wound healing Wound dressings*.

[12] Rich, N. M., Editor, S., Welling, D. R., McKay, P. L., Rasmussen, T. E., & Sam Houston, F. (2012). *HISTORICAL VIGNETTES IN VASCULAR SURGERY A brief history of the tourniquet*. https://doi.org/10.1016/j.jvs.2011.10.085

[13] Walters, T. J., Cpt, ;, Mabry, R. L., & Usa, M. C. (2005). Issues Related to the Use of Tourniquets on the Battlefield. In *MILITARY MEDICINE* (Vol. 170). Retrieved from https://academic.oup.com/milmed/article-abstract/170/9/770/4577646

[14] Mather, P. T., Luo, X., & Rousseau, I. A. (2009). *Shape Memory Polymer Research*. https://doi.org/10.1146/annurev-matsci-082908-145419

[15] Jang, L. K., Fletcher, G. K., Monroe, M. B. B., & Maitland, D. J. (2020). Biodegradable shape memory polymer foams with appropriate thermal properties for hemostatic applications. *Journal of Biomedical Materials Research Part A*, *108*(6), 1281–1294. https://doi.org/10.1002/jbm.a.36901

[16] Singhal, P., Boyle, A., Brooks, M. L., Infanger, S., Letts, S., Small, W., … Author, P. (2013). Controlling the Actuation Rate of Low-Density Shape-Memory Polymer Foams in Water NIH Public Access Author Manuscript. *Macromol Chem Phys*, *214*(11), 1204–1214. https://doi.org/10.1002/macp.201200342

[17] Landsman, T. L., Bush, R. L., Glowczwski, A., Horn, J., Jessen, S. L., Ungchusri, E., … Maitland, D. J. (2016). Design and verification of a shape memory polymer peripheral occlusion device. *Journal of the Mechanical Behavior of Biomedical Materials*, *63*, 195–206. https://doi.org/10.1016/j.jmbbm.2016.06.019

[18] Ortega, J. M., Hartman, J., Rodriguez, J. N., & Maitland, D. J. (n.d.). *Virtual Treatment of Basilar Aneurysms Using Shape Memory Polymer Foam*. https://doi.org/10.1007/s10439-012-0719-9

[19] Kragh, J. F., Aden, J. K., Steinbaugh, J., Bullard, M., & Dubick, M. A. (2015). Gauze vs XSTAT in wound packing for hemorrhage control. *American Journal of Emergency Medicine*, *33*(7), 974–976. https://doi.org/10.1016/j.ajem.2015.03.048

[20] Cannon, R. D., Wagner, M., & Jacoby, J. L. (2014). A manikin model for study of wound-packing interventions to control out-of-hospital hemorrhage. *Correspondence / American Journal of Emergency Medicine*, *32*, 1125–1147. https://doi.org/10.1016/j.ajem.2014.05.011

[21] Zwislewski, A., Nanassy, A. D., Meyer, L. K., Scantling, D., Jankowski, M. A., Blinstrub, G., & Grewal, H. (2019). Practice makes perfect: The impact of Stop the Bleed training on hemorrhage control knowledge, wound packing, and tourniquet application in the workplace. *Injury*, *50*(4), 864–868. https://doi.org/10.1016/j.injury.2019.03.025

[22] Food and Drug Administration. (2019). Consumers (Medical Devices) | FDA. Retrieved April 8, 2020, from https://www.fda.gov/medical-devices/resources-you-medical-devices/consumers-medical-devices

[23] Van Norman, G. A. (2016). Drugs, Devices, and the FDA: Part 2: An Overview of Approval Processes: FDA Approval of Medical Devices. *JACC: Basic to Translational Science*, *1*(4), 277–287. https://doi.org/10.1016/j.jacbts.2016.03.009

[24] Alzheimer Europe. (2009). Phases of clinical trials - Clinical trials - Understanding dementia research - Research - Alzheimer Europe. Retrieved April 8, 2020, from https://www.alzheimer-europe.org/Research/Understanding-dementia-research/Clinical-trials/Phases-of-clinical-trials

[25] ProCon.Org. (2020). Animal Testing - Pros & Cons - ProCon.org. Retrieved April 8, 2020, from https://animal-testing.procon.org/

[26] Akhtar, A. (2015). The Flaws and Human Harms of Animal Experimentation. *Cambridge Quarterly of Healthcare Ethics*, *24*, 407–419. https://doi.org/10.1017/S0963180115000079

[27] National Institute of Environmental Health Sciences. (2019). Alternatives to Animal Testing. Retrieved April 8, 2020, from https://www.niehs.nih.gov/health/topics/science/sya-iccvam/index.cfm

[28] Holcomb, J. B., Tilley, B. C., Baraniuk, S., Fox, E. E., Wade, C. E., Podbielski, J. M., … Van Belle, G. (2015). Transfusion of plasma, platelets, and red blood cells in a 1:1:1 vs a 1:1:2 ratio and mortality in patients with severe trauma: The PROPPR randomized clinical trial. *JAMA - Journal of the American Medical Association*, *313*(5), 471–482. https://doi.org/10.1001/jama.2015.12

[29] Pusateri, A. E., Delgado, A. V, Dick, E. J., Martinez, R. S., Holcomb, J. B., & Ryan, K. L. (2004). Application of a granular mineral-based hemostatic agent (QuikClot) to reduce blood loss after grade V liver injury in swine. *The Journal of Trauma*, *57*(3), 555–562; discussion 562. https://doi.org/10.1097/01.ta.0000136155.97758.cd

[30] Tinkoff, G., Esposito, T. J., Reed, J., Kilgo, P., Fildes, J., Pasquale, M., & Meredith, J. W. (2008). American Association for the Surgery of Trauma Organ Injury Scale I: Spleen, Liver, and Kidney, Validation Based on the National Trauma Data Bank. *Journal of the American College of Surgeons*, *207*(5), 646–655. https://doi.org/10.1016/j.jamcollsurg.2008.06.342

[31] Kashani, J., & Shih, R. D. (n.d.). *S Salicylate Overdose*. https://doi.org/10.1007/978-3-642-00418-6

[32] Rodriguez, J. N., Clubb, F. J., Wilson, T. S., Miller, M. W., Fossum, T. W., Hartman, J., … Maitland, D. J. (2014). *In vivo* response to an implanted shape memory polyurethane foam in a porcine aneurysm model. *Journal of Biomedical Materials Research Part A*, *102*(5), 1231–1242. https://doi.org/10.1002/jbm.a.34782

[33] Kragh, J. F., Aden, J. K., Steinbaugh, J., Bullard, M., & Dubick, M. A. (2015). Gauze vs XSTAT in wound packing for hemorrhage control. *American Journal of Emergency Medicine*, *33*(7), 974–976. https://doi.org/10.1016/j.ajem.2015.03.048

[34] Fabre, J.W. & Grehan, A & Whitehorne, Michael & Sawyer, Greta & Dong, X & Salehi, S & Eckley, L & Zhang, X & Seddon, M & Shah, A.M. & Davenport, Mark & Rela, Mohamed. (2008). Hydrodynamic gene delivery to the pig liver via an isolated segment of the inferior vena cava. Gene therapy. 15. 452-62. 10.1038/sj.gt.3303079.

[35] Lautt WW. Hepatic Circulation: Physiology and Pathophysiology. San Rafael (CA): Morgan & Claypool Life Sciences; 2009. Chapter 2, Overview. Available from: https://www.ncbi.nlm.nih.gov/books/NBK53069/

[36] Wang, Z., Volinsky, A. A., & Gallant, N. D. (2014). Crosslinking Effect on Polydimethylsiloxane Elastic Modulus Measured by Custom-Built Compression Instrument. *J. Appl. Polym. Sci*, 41050. https://doi.org/10.1002/app.41050

[37] Yeh, Wen-Chun & Jeng, Yung-Ming & Hsu, Hey-Chi & Kuo, Po-Ling & Li, Meng-Lin & Yang, Pei & Lee, Chii-Ming & Li, Pai-Chi. (2001). Young's modulus measurements of human liver and correlation with pathological findings. Proceedings of the IEEE Ultrasonics Symposium. 2. 1233 - 1236 vol.2. 10.1109/ULTSYM.2001.991942.

[38] Pasumarthy, R. K. A., & Tippur, H. V. (2016). *Test Method Mechanical and optical characterization of a tissue surrogate polymer gel*. https://doi.org/10.1016/j.polymertesting.2016.08.004

Nakira Christmas

407 Small Road Apt 317D▪ Syracuse, NY 13210 ▪ (503) 419-7746 ▪ nchristm@syr.edu

Objective:

To obtain a biotechnological career opportunity in order to utilize skills I have obtained from shape memory polymers research, bioengineering course work, leadership development work experiences and corporate internships.

Education:

B.S. Bioengineering with minor in Electrical Engineering, Syracuse University, Syracuse NY, May 2019

- Biomedical 5 Year BS/MS Program; Anticipated Graduation Date: May, 2020
- **Cumulative G.P.A: 3.18/4.00 (Undergraduate studies)** | **3.91/4.00 (Graduate studies)**

Software Knowledge: AutoCAD, MATLAB, Autodesk Revit, Microsoft Word, Microsoft Excel, Microsoft PowerPoint, Microsoft Access, Vernier Software and Technology, Arduino, Fritzing Creator, Multisim, Image J, Scanning Electron Microscopy, Differential Scanning Calorimetry, Thermal Gravimetric Analysis

Work Experience:

Graduate Advisor, Louis Stokes Alliance for Minority Participation (LSAMP***)*** August 2019-Present

Outdoor Lighting Intern, National Grid, Syracuse, NY, May 2018-August 2019

- Worked with a small direct group and assisted in a variety of projects that would increase lighting revenue and reduce energy consumption of streetlights
- Created graphics and flyers for conferences, presentations, and informational documents
- Served as an engineering subject expert for smaller projects
- Directed robotics portion of trades camp for Syracuse City youth minorities

Community Assistant, University Village Apartments, Syracuse, NY December 2017-May 2020

- Works in a team of 5 to assist the apartment community with leasing, tours, lockouts, packages, use of amenities, and recruiting new workers once current workers graduate
- Assists managers in community building events by creating programs/formulating logistics, advertisement content, and running the event

Main Desk Assistant, Syracuse University, Syracuse, NY January 2016-May 2019

- Worked with over 1,200 residents, set timelines for key returns and package pickup
- Assist the Residence Director with postal sorting, resident lockouts, and organization of student records
- Responsible for collecting and managing lock-out funds, used for local charities, from residents

Engineering Special Program:

College of Engineering Teaching Assistant, Syracuse University, Syracuse, NY
August 2019-May 2020

- Assisted in teaching senior bioengineering laboratory
- Assisted in leading independent research opportunities with multiple groups of engineering students

Louis Stokes Alliance for Minority Participation (LSAMP), Syracuse University, Syracuse, NY, September 2017- April 2019

- Studied alongside a PhD student regarding shape memory polymers and mathematics in fluids
- Increased research reading qualities, manipulated research for own research goals as well as working in a team on a definitive timeline

Academic Excellence Workshop Facilitator, Syracuse University: College of Engineering and Computer Science, Syracuse, NY, August 2016- December 2016

- Facilitated assistance for calculus I to improve math grades for new engineering students

Leadership/Activities:

President, Alpha Kappa Alpha Sorority, Incorporated November 2016- May 2019
Technology Chair, Alpha Kappa Alpha Sorority, Incorporated November 2016- May 2019
Historian/Social Chair, National Pan Hellenic Council April 2017- September 2018
Captain, Varsity School Athletics, Syracuse University Cheerleading August 2015- May 2018

Volunteer Work:

Math Tutor, Syracuse, NY November 2016- May 2019
ASCEND, Grade Schools in Onondaga County, Syracuse, NY November 2016- May 2018
Engineering Ambassador to Middle School Students, Charles County, MD October 2013- January 2016